Rapid Covalent Ligation of Fluorescent Peptides to Water Solubilized Quantum Dots

Juan B. Blanco-Canosa,[†] Igor L. Medintz,[‡] Dorothy Farrell,[§] Hedi Mattoussi,*,[§,||] and Philip E. Dawson*,[†]

Department of Chemistry and Department of Cell Biology, The Scripps Research Institute, 10550 North Torrey Pines Road, La Jolla, California 92037, Center for Bio/Molecular Science and Engineering, U.S. Naval Research Laboratory, Washington, DC 20375, and Optical Sciences Division, U.S. Naval Research Laboratory, Washington, DC 20375

Received January 7, 2010; E-mail: dawson@scripps.edu; mattoussi@chem.fsu.edu

Abstract: Water solubilized nanoparticles such as CdSe−ZnS core−shell nanocrystals (quantum dots, QDs) have great potential in bioimaging and sensing applications due to their excellent photophysical properties. However, the efficient modification of QDs with complex biomolecules represents a significant challenge. Here, we describe a straightforward arylhydrazone approach for the chemoselective covalent modification of QDs that is compatible with neutral pH and micromolar concentrations of the peptide target. The kinetics of covalent modification can be monitored spectroscopically at 354 nm in the presence of the QD and average peptide/QD ratios from 2:1 to 11:1 were achieved with excellent control over the desired valency. These results suggest that aniline catalyzed hydrazone ligation has the potential to provide a general method for the controlled assembly of a variety of nanoparticle-biomolecule hybrids.

Introduction

The efficient functionalization of nanoparticles (NPs) is an ongoing challenge in nanotechnology. Although semiconductor nanocrystals (quantum dots, QDs) and metallic nanoparticles have great potential in a variety of technical applications, much of their utility requires specific interactions with surfaces, organic materials, or biological macromolecules. In particular, luminescent QDs have great potential in biological imaging and sensing applications due to their excellent photophysical properties that include high quantum yields, large Stokes shifts, broad absorption spectra, low levels of photobleaching, long luminescent lifetimes, and photoluminescent (PL) emissions that are narrow, symmetric, and size-tunable.[1−6] In aqueous media, the hydrophobic semiconducting CdSe−ZnS core−shell quantum dots can be solubilized through coating with amphiphilic block copolymers[7−10] or acidic thiol ligands such as mercaptoacetic

acid[11,12] and dihydrolipoic acid (DHLA).[13] Recently, the use of hydrophilic polyethyleneglycol (PEG) appended-thiols[14,15] has produced highly water-soluble QDs that can be terminally functionalized with amines or carboxylic acids to facilitate nonselective labeling with functional groups present on biomolecules.[15] In addition, QDs can be capped with polyCys[16−18] or polyHis[19] (His$_6$ tag) peptide sequences. In particular, His$_6$ sequences have been shown to bind the ZnS shell in DHLA

[†] The Scripps Research Institute.
[‡] Center for Bio/Molecular Science and Engineering, U.S. Naval Research Laboratory.
[§] Optical Sciences Division, U.S. Naval Research Laboratory.
[||] Present address: Department of Chemistry, Florida State University, Tallahassee, FL 32306.

(1) Alivisatos, A. P. *Science* **1996**, *271*, 933−937.
(2) Dabbousi, B. O.; RodriguezViejo, J.; Mikulec, F. V.; Heine, J. R.; Mattoussi, H.; Ober, R.; Jensen, K. F.; Bawendi, M. G. *J. Phys. Chem. B* **1997**, *101*, 9463−9475.
(3) Bruchez, M.; Moronne, M.; Gin, P.; Weiss, S.; Alivisatos, A. P. *Science* **1998**, *281*, 2013−2016.
(4) Medintz, I. L.; Uyeda, H. T.; Goldman, E. R.; Mattoussi, H. *Nat. Mater.* **2005**, *4*, 435−446.
(5) Bailey, R. E.; Smith, A. M.; Nie, S. M. *Physica E* **2004**, *25*, 1−12.
(6) Michalet, X.; Pinaud, F. F.; Bentolila, L. A.; Tsay, J. M.; Doose, S.; Li, J. J.; Sundaresan, G.; Wu, A. M.; Gambhir, S. S.; Weiss, S. *Science* **2005**, *307*, 538−544.
(7) Gerion, D.; Pinaud, F.; Williams, S. C.; Parak, W. J.; Zanchet, D.; Weiss, S.; Alivisatos, A. P. *J. Phys. Chem. B* **2001**, *105*, 8861−8871.

(8) Dubertret, B.; Skourides, P.; Norris, D. J.; Noireaux, V.; Brivanlou, A. H.; Libchaber, A. *Science* **2002**, *298*, 1759−1762.
(9) Wu, X. Y.; Liu, H. J.; Liu, J. Q.; Haley, K. N.; Treadway, J. A.; Larson, J. P.; Ge, N. F.; Peale, F.; Bruchez, M. P. *Nat. Biotechnol.* **2003**, *21*, 41−46.
(10) Pellegrino, T.; Manna, L.; Kudera, S.; Liedl, T.; Koktysh, D.; Rogach, A. L.; Keller, S.; Radler, J.; Natile, G.; Parak, W. J. *Nano Lett.* **2004**, *4*, 703−707.
(11) Chan, W. C. W.; Nie, S. M. *Science* **1998**, *281*, 2016−2018.
(12) Ding, S. Y.; Jones, M.; Tucker, M. P.; Nedeljkovic, J. M.; Wall, J.; Simon, M. N.; Rumbles, G.; Himmel, M. E. *Nano Lett.* **2003**, *3*, 1581−1585.
(13) Mattoussi, H.; Mauro, J. M.; Goldman, E. R.; Anderson, G. P.; Sundar, V. C.; Mikulec, F. V.; Bawendi, M. G. *J. Am. Chem. Soc.* **2000**, *122*, 12142−12150.
(14) Uyeda, H. T.; Medintz, I. L.; Jaiswal, J. K.; Simon, S. M.; Mattoussi, H. *J. Am. Chem. Soc.* **2005**, *127*, 3870−3878.
(15) (a) Susumu, K.; Uyeda, H. T.; Medintz, I. L.; Pons, T.; Delehanty, J. B.; Mattoussi, H. *J. Am. Chem. Soc.* **2007**, *129*, 13987−13996. (b) Liu, W.; Howarth, M.; Greytak, A. B.; Zheng, Y.; Nocera, D. G.; Ting, A. Y.; Bawendi, M. G. *J. Am. Chem. Soc.* **2008**, *130*, 1274−1284.
(16) Pinaud, F.; King, D.; Moore, H. P.; Weiss, S. *J. Am. Chem. Soc.* **2004**, *126*, 6115−6123.
(17) Akerman, M. E.; Chan, W. C. W.; Laakkonen, P.; Bhatia, S. N.; Ruoslahti, E. *Proc. Natl. Acad. Sci. U.S.A.* **2002**, *99*, 12617−12621.
(18) Gomez, N.; Winter, J. O.; Shieh, F.; Saunders, A. E.; Korgel, B. A.; Schmidt, C. E. *Talanta* **2005**, *67*, 462−471.
(19) Sapsford, K. E.; Pons, T.; Medintz, I. L.; Higashiya, S.; Brunel, F. M.; Dawson, P. E.; Mattoussi, H. *J. Phys. Chem. C* **2007**, *111*, 11528−11538.

Scheme 1. General Strategy Followed for the Ligation of Peptides to PEGylated QDs[a]
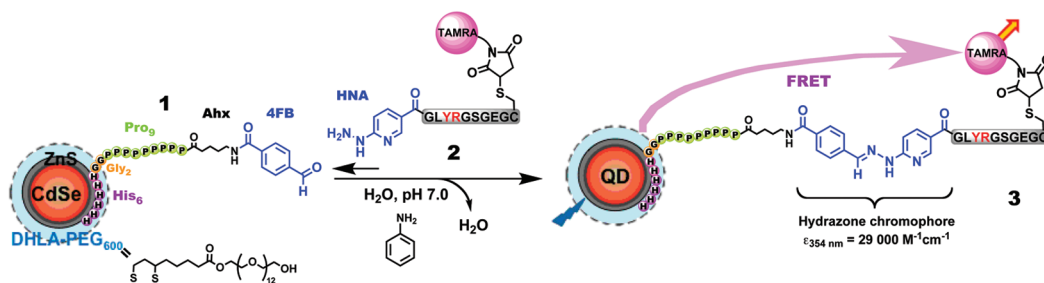
[a] Peptide **2** is ligated to QD/peptide **1** to yield the QD/peptide **3** product. The highlighted Y and R residues in peptide **3** are subsequently cleaved by addition of the proteases chymotrypsin or trypsin.

and DHLA-PEG capped QDs with high affinity, making them an attractive approach to introduce functional groups into QDs.

Several strategies have been developed to introduce biological molecules onto the surface of QDs. For example, commercial streptavidin decorated QDs have been used to bind biotin linked labels,[20,21] and positively charged proteins have been shown to bind negatively charged acidic QDs through electrostatic interactions.[13] However, these approaches are limited in utility, as they require a large protein to mediate the binding interaction. In contrast, covalent labeling enables a direct link to the solubilizing caps of the QD to be achieved. The most commonly used method is amide bond formation between carboxylic acids and amines,[3,7,8,11,15,22−24] an approach that requires a significant excess of label and typically suffers from poor chemoselectivity, and a high degree of cross-linking.[4,13,24] Recently, the use of a PEG-EDC coupling reagent that reduces cross-linking and aggregation in aqueous systems was reported.[24] Alternatively, cysteine-maleimide reactions have found utility in peptide−QD conjugation.[25,26]

Despite significant advances in QD functionalization in aqueous solution, the efficient covalent modification of QDs and other NPs remains a significant technical challenge. While QDs are typically handled at micromolar concentrations, most conjugation reactions use a large excess of label (mM), which limits the efficiency of the process.[27] In addition, since analytical methods are not available to rapidly characterize NP/peptide conjugates, these reactions are typically performed without direct feedback on the progress of the reaction. As a result, there is a need for the development of coupling strategies that can achieve enhanced reaction kinetics while maintaining chemoselectivity. Peptides are especially attractive molecules for QD modification since they bind selectively to numerous important targets and can be generated synthetically in a straightforward manner.[28]

These properties make them good candidates for cellular delivery, sensing applications, and drug therapy.

Approach

The generation of peptide−QD complexes would be greatly facilitated by the development of a robust and convergent approach for the direct chemical conjugation of fluorescent peptide substrates directly to a reactive nanoparticle (Scheme 1). Ideally, such a method would allow unprotected peptides to be conjugated chemoselectively and without requiring an excess of peptide. Recently, we described an approach to accelerate hydrazone ligations[29,30] by the nucleophilic catalyst aniline.[31] The high chemoselectivity of the hydrazone reaction in neutral aqueous buffer enables the conjugation of peptides to carbohydrates on cell surfaces.[32,33] Such enhanced reaction rates, especially at neutral pH, suggested that this hydrazone-based approach might be utilized for the controlled and efficient assembly of peptides to nanoparticles such as QDs.

The reaction of a 4-formylbenzoyl group (*4FB*) and a 2-hydrazinonicotinoyl group (*HYNIC*) is advantageous since it yields a highly conjugated hydrazone product that has a clear optical signature with $\varepsilon_{354nm} = 29\,000$ M^{-1} cm^{-1} (Scheme 1).[34,35] In addition, the high reaction rate at pH 7.0 (170 M^{-1} s^{-1})[36] enables the efficient coupling and labeling of biomolecules at micromolar concentrations and neutral pH. To introduce the required functional groups onto the DHLA-PEG$_{600}$ QDs, we designed a peptide with a benzaldehyde reactant and a His$_6$ QD surface binding domain, separated by a polyproline spacer to extend the reactive aldehyde away from the NP/PEG surface. Specifically, the peptide, *4FB*-Ahx-Pro$_9$Gly$_2$His$_6$ (*4FB* = 4-formylbenzaldehyde, Ahx = Amino-hexanoyl), utilizes an Ahx-Pro$_9$Gly$_2$-linker in which the Pro$_9$ is expected to form a Proline type II helix extending ∼3 nm from the QD/PEG surface.[37,38] This approach allows considerable control over the

(20) Howarth, M.; Takao, K.; Hayashi, Y.; Ting, A. Y. *Proc. Natl. Acad. Sci. U.S.A.* **2005**, *102*, 7583–7588.
(21) Prinzen, L.; Miserus, R. J. J. H. M.; Dirksen, A.; Hackeng, T. M.; Deckers, N.; Bitsch, N. J.; Megens, R. T. A.; Douma, K.; Heemskerk, J. W.; Kooi, M. E.; Frederik, P. M.; Slaaf, D. W.; van Zandvoort, M. A. M. J.; Reutelingsperger, C. P. M. *Nano Lett.* **2007**, *7*, 93–100.
(22) Gao, X. H.; Cui, Y. Y.; Levenson, R. M.; Chung, L. W. K.; Nie, S. M. *Nat. Biotechnol.* **2004**, *22*, 969–976.
(23) Clapp, A. R.; Goldman, E. R.; Mattoussi, H. *Nat. Protoc.* **2006**, *1*, 1258–1266.
(24) Shen, H. Y.; Jawaid, A. M.; Snee, P. T. *ACS Nano* **2009**, *3*, 915–923.
(25) Zhou, M.; Nakatani, E.; Gronenberg, L. S.; Tokimoto, T.; Wirth, M. J.; Hruby, V. J.; Roberts, A.; Lynch, R. M.; Ghosh, I. *Bioconjugate Chem.* **2007**, *18*, 323–332.
(26) Chen, Y.; Thakar, R.; Snee, P. T. *J. Am. Chem. Soc.* **2008**, *130*, 3744–3745.
(27) Dirksen, A.; Dawson, P. E. *Curr. Opin. Chem. Biol.* **2008**, *12*, 760–766.
(28) Zhou, M.; Ghosh, I. *Biopolymers* **2007**, *88*, 325–339.

(29) Dirksen, A.; Hackeng, T. M.; Dawson, P. E. *Angew. Chem., Int. Ed.* **2006**, *45*, 7581–7584.
(30) Dirksen, A.; Dirksen, S.; Hackeng, T. M.; Dawson, P. E. *J. Am. Chem. Soc.* **2006**, *128*, 15602–15603.
(31) Cordes, E. H.; Jencks, W. P. *J. Am. Chem. Soc.* **1962**, *84*, 826–831.
(32) Zeng, Y.; Ramya, T. N. C.; Dirksen, A.; Dawson, P. E.; Paulson, J. C. *Nat. Methods* **2009**, *6*, 207–209.
(33) Nauman, D. A.; Bertozzi, C. R. *Biochim. Biophys. Acta* **2001**, *1568*, 147–154.
(34) Schwartz, D. A. (Solulink Biosciences, Inc.) U.S. Patent 6, 800, 728, 2004.
(35) Flavell, R. R.; Kothari, P.; Bar-Dagan, M.; Synan, M.; Vallabhajosula, S.; Friedman, J. M.; Muir, T. W.; Ceccarini, G. *J. Am. Chem. Soc.* **2008**, *130*, 9106–9112.
(36) Dirksen, A.; Dawson, P. E. *Bioconjugate Chem.* **2008**, *19*, 2543–2548.
(37) Stryer, L.; Haugland, R. P. *Proc. Natl. Acad. Sci. U.S.A.* **1967**, *58*, 719–726.

number of aldehyde groups displayed on each QD through the molar ratio added,[19] and is also compatible with commercially available QD preparations.[39] In addition, the *4FB*/aldehyde is easily introduced into the capping peptide using established chemistries (Scheme 1).[36] Similar to the dithiol capping groups, the His[6] tag interacts directly with the ZnS surface shell with high affinity (K_d ~1 nM).[19] To validate the approach, a protease substrate peptide **2** (*HYNIC*-GLYRGSGEGC-TAMRA) was designed to incorporate both a *HYNIC* hydrazine ligation handle and a Cys/maleimide linked TAMRA fluorophore. These QD-peptide conjugates were designed to act as fluorescently quenched protease substrates,[40] since the TAMRA fluorophore is a known FRET acceptor for QDs.[41−43]

Experimental Procedures

Materials and Methods. All solvents and chemicals were purchased from commercial sources and used without further purification: DMF (HPLC grade) from OmniSolv, CH_2Cl_2 from Fisher, TFA (trifluoroacetic acid, Biograde) from Halocarbon, CH_3CN from J. T. Baker. Water was purified using a Millipore Milli-Q water purification system. DIEA (*N,N*-diisopropylethylamine) and 4-formyl-benzoic acid (*4FB*) were from Sigma-Aldrich, HCTU (*o*-(1-benzotriazol-1-yl)-1,1,3,3-tetramethyluronium hexafluorophosphate) and HOBt (1-hydroxybenzotriazole) from Peptides International, HATU (*o*-(7-azabenzotriazol-1-yl)-1,1,3,3-tetramethyluronium hexafluorophosphate) and Tetramethylrhodamine-5-(and-6)-maleimide from Anaspec, 6-Boc-hydrazinonicotinic acid (6-Boc-HYNIC) from Solulink Biosciences and amino acids from CS Bio. Peptides were purified by reverse phase HPLC (RP-HPLC). Analytical HPLC was carried out in a Varian ProStar Model 210 equipped with a Dynamax Absorbance Rainin Detector. Analytical injections were monitored at 220 nm. Separations were performed using an Einstein C-18 cartridge (65 × 15 mm) at a flow rate of 2 mL/min with a gradient from 0 to 67% of B in 30 min (eluent A, 0.1% TFA/H_2O; eluent B, 0.09% TFA in 90% CH_3CN/H_2O). Preparative HPLC was performed in a Waters Delta Prep 4000 equipped with a Gilson UV detector model 116 and a Phenomenex column (10 μm, 90 Å, 250 × 21.20 mm) at a flow rate of 15 mL/min employing the following gradient: 0 → 85 min, 0 → 70% of B. Preparative injections were monitored at 220 nm. Peptides were desalted prior their use with OPC Oligonucleotide Purification Cartridge (Applied Biosystems).[19]

Peptides were characterized using electrospray ionization MS on a LC/MS API *I* Plus quadrupole mass spectrometer (Sciex). Peptides masses were calculated from the experimental mass to charge (*m/z*) ratios from all of the observed protonation states of a peptide by using the MacSpec software (Sciex).

UV measurements were undertaken in a Genesys 6 UV/vis spectrometer (Thermo Electron Corporation). Fluorescence was performed in a Tecan Safire Monochromator Plate Reader (Tecan, Research Triangle Park, NC).

Peptide Synthesis. Peptides were synthesized manually using *in situ* neutralization cycles for Boc-solid-phase-peptide synthesis (Boc-SPPS) following procedures described in the literature.[44] Peptides were synthesized on 0.1 mmol MBHA resin (4-Methylbenzhydrylamine, Peptides International, 0.65 mmol/g) using 1.0 mmol of amino acid, 1.0 mmol of HCTU/HOBt (in a 0.4 M solution

in DMF 1:1, and 2 mmol of DIEA. Coupling times were 1 h. Following chain assembly, peptides were cleaved from the resin with HF and 10% of anisole for 1 h at 0 °C.

Synthesis of *4FB*-Ahx-Pro₉Gly₂His₆ Peptide 1. 4-Formylbenzoyl (*4FB*) was coupled to Ahx-Pro₉Gly₂His₆ (12 mg, 6.2×10^{-3} mmol) in a H_2O/CH_3CN solution (5 mL, 1:1) using succinimidyl 4-formylbenzoate (2.3 mg, 9.3×10^{-3} mmol, 1.5 equiv) and DIEA (7 equiv) yielding 11.5 mg of **1** (90%).

Synthesis of *HYNIC*-GLYRGSGEGC-TAMRA Peptide 2. 6-Boc-hydrazinonicotinic acid (Boc-HYNIC) was activated with HATU (0.15 mmol) and DIEA (0.23 mmol) in DMF (1.5 mL) for 2.5 min and then added over the resin (0.1 mmol). Labeling with TAMRA (*N,N,N′,N′*-Tetramethylrhodamine) was carried out by reacting the cysteinyl peptide (5.5 mg, 4.8×10^{-3}, 1.5 equiv) with (5,6)-Maleimide TAMRA (2 mg, 4.1×10^{-3}, 1 equiv) in 10 mM Tris·HCl, pH 7.5, 100 mM NaCl buffer. A total of 1.8 and 3.2 mg of each isomer were obtained after HPLC purification (76% both isomers).

Quantum Dot Synthesis. Quantum Dots made of CdSe and coated with a ZnS shell with an inorganic core of about 2.8 nm were synthesized according procedures previously reported.[2] Following the synthesis, TOP/TOPO (trioctyl phosphine/trioctyl phosphine oxide) ligands were exchanged with DHLA-PEG₆₀₀ in methanol solution under N_2 atmosphere.[14]

Peptide/QD Ligation. QDs (~1 μM) were first incubated with His₆ bearing peptides **1** (15−30 μM) for 30 min at room temperature in 50−100 mM HEPES buffer pH 7.0 (350 μL total volume). Then, hydrazine-TAMRA peptide **2** was added at the desired concentration and, finally, neat aniline (~100 mM). Ligation reactions were carried out in 0.5 mL quartz cuvettes when monitored at 354 nm or in eppendorf tubes.

Reactions were conducted over 5 h and then filtered through PD-10 columns (GE Healthcare, 2.5 mL void volume) using 10 mM sodium phosphate buffer pH 7.5 as eluting buffer. The first fraction (1 mL) was collected and the absorbance at 354 and 555 nm was measured, affording the number of peptides **2** ligated per QD ($\varepsilon_{350nm} = 520\,000$ M^{-1} cm^{-1}). The 555 nm absorbance is unique to TAMRA fluorophore ($\varepsilon_{555nm} = 65\,000$ M^{-1} cm^{-1}) allowing its concentration to be determined as well as the equimolar bisarylhydrazone group in all ligated peptides. Using these values, the QD concentration was determined by measuring the absorbance at 354 nm and subtracting components attributed to the bisarylhydrazone and TAMRA chromophores (bisarylhydrazone $\varepsilon_{354nm} = 29\,000$ M^{-1} cm^{-1} and TAMRA ε_{354nm} is 11% of the value at 555 nm). Predicted loadings for **3** were estimated using $K_{eq} = 2.3 \times 10^6$ M^{-1}.[36]

Fluorescence and FRET Analysis. For fluorescence analysis samples were transferred to a 96-well microtiter plate, excited at 300 nm, and fluorescence spectra were collected. FRET efficiency $E(n)$ (n = number of TAMRA acceptors per QD) was determined according the following equation:

$$E(n) = \frac{F_D - F_{DA}}{F_D} \tag{1}$$

where F_D and F_{DA} represent the fluorescence intensities of the donor in the absence and presence of n dye acceptors (number of dye labeled peptide **2** ligated per QD), respectively.[45] Using the Förster theory and data from FRET efficiency, distance r from center-to-center (QD-to-TAMRA) was calculated:

(38) Arora, P. S.; Ansari, A. Z.; Best, T. P.; Ptashne, M.; Dervan, P. B. *J. Am. Chem. Soc.* **2002**, *124*, 13067−13071.

(39) Dennis, A. M.; Bao, G. *Nano Lett.* **2008**, *8*, 1439−1445.

(40) Medintz, I. L.; Clapp, A. R.; Brunel, F. M.; Tiefenbrunn, T.; Uyeda, H. T.; Chang, E. L.; Deschamps, J. R.; Dawson, P. E.; Mattoussi, H. *Nat. Mater.* **2006**, *5*, 581−589.

(41) Willard, D. M.; Carrillo, L. L.; Jung, J.; van Orden, A. *Nano Lett.* **2001**, *1*, 469−474.

(42) Medintz, I. L.; Konnert, J. H.; Clapp, A. R.; Stanish, I.; Twigg, M. E.; Mattoussi, H.; Mauro, J. M.; Deschamps, J. R. *Proc. Natl. Acad. Sci. U.S.A.* **2004**, *101*, 9612−9617.

(43) Shi, L.; De Paoli, V.; Rosenzweig, N.; Rosenzweig, Z. *J. Am. Chem. Soc.* **2006**, *128*, 10378−10379.

(44) Schnolzer, M.; Alewood, P.; Jones, A.; Alewood, D.; Kent, S. B. *Int. J. Pept. Protein Res.* **1992**, *40*, 180−193.

(45) Lakowicz, J. R. *Principles of Fluorescence Spectroscopy*, 3rd ed.; Springer: New York, 2006.

$$r = R_0(n(1 - E)/E)^{1/6} \qquad (2)$$

where R_0 is the Förster distance corresponding to a 50% energy transfer efficiency.[45] The experimental data are analyzed using a corrected FRET efficiency where effects of heterogeneity in the conjugate valence are taken into account via the Poison distribution function $p(k,n)$.[40,46] The corrected FRET efficiency was rewritten as:

$$E(n) = \sum_{k=1}^{n} p(k, n)E(k) \quad \text{and} \quad p(k, n) = \frac{e^{-n}n^k}{k!} \qquad (3)$$

where n is the nominal average ratio of peptides **2** per QD mixed in solution and k is the exact number of peptides **2** conjugated to the QD/**1** complexes.

The corrected values were used to provide calibration curves that were used in the enzymatic assays.

Enzymatic Assays. α-Chymotrypsin from bovine pancreas (specific activity of 60 units/mg) and trypsin from bovine pancreas (specific activity of 10 000−15 000 BAEE units/mg of protein) were purchased from Sigma-Aldrich. For inhibition assays, ovomucoid trypsin inhibitor (Sigma-Aldrich) with a specific activity of 1 mg inhibits 0.8−1.2 mg of trypsin was used.

QD−peptide **3** conjugates with different ratios of ligated peptide were used to obtain a standard curve, as described.[40] For all samples, the dispersions were subjected to gel filtration to remove excess aniline prior to peforming the proteolytic assays. QD/peptide substrates (1:11, 0.1 μM QDs) were exposed to increasing concentrations of α-chymotrypsin (0.15−20 μM) and trypsin (0.04−42 μM) in 0.5× PBS buffer pH 7.5 at 30 °C for 10 min incubations. The reactions were quenched with the addition of the alkylating agent α-iodoacetamide (final concentration 0.36 mg/mL), and changes in the FRET signature were monitored by tracking the QD emission at 537 nm (peak emission). Under these conditions, initial proteolytic rates could be measured. Comparison of the values from the QD PL following proteolysis with the calibration curves enables us to infer the number of QD/peptide complex that are intact and to transform the FRET recovery signal to velocity units. Using standard Michaelis−Menten kinetic analysis for excess enzyme conditions, maximal apparent velocity $V_{\text{max.app.}}$ and the apparent Michaelis constant $K_{\text{Mapp.}}$ were determined.[47]

$$V_{\text{app.}} = \frac{d[P]}{dt} = \frac{V_{\text{max.app.}}[E]}{K_{\text{Mapp.}} + [E]} \qquad (4)$$

where [P] and [E] designate the product (digested substrate) and enzyme concentrations, respectively. The inhibitor dissociation constant K_i was calculated assuming a competitive inhibition mechanism (ovamucoid trypsin inhibitor (I) is known to act competitively):

$$V_{\text{app.}}^i = \frac{d[P]}{dt} = \frac{V_{\text{max.app.}}^i[E]}{K_{\text{Mapp.}}^i + [E]} \qquad (5)$$

where $V_{\text{max.app.}}^i$ and $K_{\text{Mapp.}}^i$ correspond to the Michaelis−Menten parameters in the presence of an inhibitor. Assuming that $K_{\text{Mapp.}}^i \sim K_{\text{Mapp.}}$, then the K_i can be derived from:

$$V_{\text{max.app.}}^i = \frac{V_{\text{max.app.}}}{(1 + [I]/K_i)} \qquad (6)$$

Agarose Gel Electrophoresis. QDs (∼1 μM) were assembled with *4FB*-Ahx-Pro$_9$Gly$_2$His$_6$ (∼15 equiv) and several equivalents

(46) Pons, T.; Medintz, I. L.; Wang, X.; English, D. S.; Mattoussi, H. *J. Am. Chem. Soc.* **2006**, *128*, 15324−15331.

(47) Bowden, A. C. *Fundamentals of Enzyme Kinetics*; Revised Ed.; Portland Press Ltd.: London, 1995.
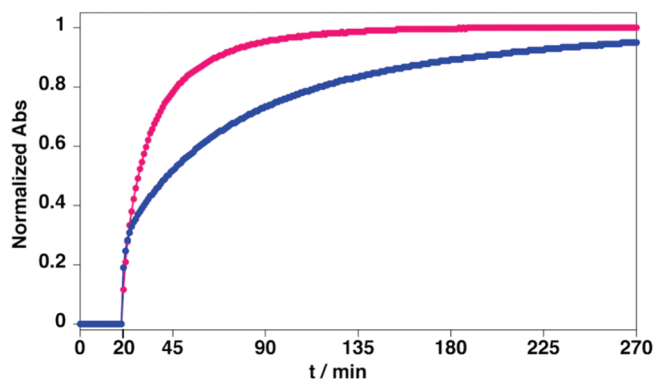
Figure 1. UV monitoring of the chemical ligations. (Blue circles): between **1** (21 μM) self-assembled to QDs (0.9 μM) and **2** (14 μM) in presence of ∼100 mM of aniline. (Red circles): between **1** (22 μM) and **2** (14.9 μM) in presence of 100 mM of aniline and absence of QDs. Aniline was added to reaction mixtures at 20 min. Note that the contributions from the QDs and TAMRA to the absorption has been subtracted before normalization.

of peptide *HYNIC*-GLYRGSGEGC-TAMRA were ligated (0, 2, 4, 6, 8, 12 or 16). Reactions were carried out in 50−100 mM HEPES pH 7.0 and ∼100 mM aniline for 5 h. Then, they were filtered through PD-10 columns (GE Healthcare) using 10 mM sodium phosphate buffer pH 7.5 and the absorbance at 354 and 555 nm was registered affording the number of peptides **2** ligated per QD. Finally, ∼20 pmol of QDs (∼0.5 μM) conjugated with TAMRA ligated peptides was mixed with loading buffer (30% glycerol in H$_2$O, no staining dyes), loaded into 2% agarose gel, and run in 1× TBE (90 mM Tris borate, 2 mM EDTA, pH 8.3) buffer at ∼10 V/cm for 10 to 20 min. Fluorescent images were collected on a Kodak 440 Digital Image Station (Rochester, NY) using 365 nm excitation and long-pass cutoff filters at 523 or 590 nm.

Results and Discussion

Assembly of Benzaldehyde Functionalized QDs. Water solubilized DHLA-PEG$_{600}$ QDs (537 nm emission) were modified with synthetic peptide **1** (*4FB*-Ahx-Pro$_9$Gly$_2$His$_6$) using the established method of direct His tag binding to the ZnS QD surface.[19] They will be referred to as *4FB*-**1**-QDs. It has been shown that His$_6$ binding domain enables not only a strong and rapid binding to the NPs, but also the controlled functionalization of up to ∼50 His$_6$ peptides per ZnS shell.[40,48−50] To test the utility of aniline catalyzed hydrazone ligation for the covalent modification of QDs, we self-assembled ∼1 μM QD with between 15 and 30 copies of **1** (15−30 μM) depending on the individual experiment. Although the QD nanoparticles can accommodate larger numbers of peptides, this lower loading ensured a quantitative loading of the His$_6$ peptides.[48] The resulting concentrations of displayed peptide were ∼15−30 μM and are consistent with concentrations frequently encountered when handling biological molecules and NPs.

Direct Monitoring of Peptide−QD Ligation by UV/vis. The ligation reaction was initiated by adding *HYNIC* peptide **2** (14 μM, pH 7.0, 23 °C) to the *4FB*-**1**-QDs (0.9 μM QDs, 21 μM **1**). As shown in Figure 1, the hydrazone reaction is very slow at pH 7.0 in the absence of aniline catalyst (Figure 1, blue

(48) Prasuhn, D. E.; Deschamps, J. R.; Susumu, K.; Stewart, M. H.; Boeneman, K.; Blanco-Canosa, J. B.; Dawson, P. E.; Medintz, I. L. *Small* **2010**, *6*, 555−564.

(49) Medintz, I. L.; Clapp, A. R.; Mattoussi, H.; Goldman, E. R.; Fisher, B.; Mauro, J. M. *Nat. Mater.* **2003**, *2*, 630−638.

(50) Delehanty, J. B.; Medintz, I. L.; Pons, T.; Brunel, F. M.; Dawson, P. E.; Mattoussi, H. *Bioconjugate Chem.* **2006**, *17*, 920−927.

Table 1. Ratio of Peptide **3** per QD Achieved by Incubating *4FB*-**1**-QD (15:1) with Increasing Equivalents of Peptide **2** ($K_{eq} = 2.3 \times 10^6$ M^{-1}) in the Presence of Aniline ($\sim$100 mM)

[QD] (μM)	[1] (μM)	[2] (μM)	ratio 3/QD (predicted)	ratio 3/QD (observed)
1.1	16.5	0	0	0
1.1	16.5	2.2	1.9	1.9 (100%)
1.1	16.5	4.4	3.9	3.9 (100%)
1.1	16.5	8.8	7.6	6.0 (79%)
1.1	16.5	13.2	11.0	11.0 (100%)

circles, $t = 0$ to 20 min) as monitored by hydrazone chromophore formation (the ligation rate constant at pH 7 is less than 1. 0 M^{-1} s^{-1}).[36] Addition of $\sim$100 mM aniline at $t = 20$ min dramatically increased hydrazone product formation, approaching equilibrium after $\sim$4 h. When compared to the reaction in the absence of quantum dots (Figure 1, red circles) the reaction appears to proceed at a similar rate for the first 30% of the reaction ($\sim$5 min) and subsequently proceeds at a slightly slower rate. This profile is consistent with an increase in steric hindrance as the QDs become highly functionalized. Nevertheless, the QD reaction does approach a similar level of total conjugation ($\sim$90% of the added peptide **2** is conjugated) in the 4 h time window shown. This demonstrates that a high yielding, covalent conjugation of peptides to hydrophilic QDs can be achieved. It should be noted that, since the hydrazone ligation is reversible, a maximal conversion of 95% was expected based on $K_{eq} = 2.3 \times 10^6$ M^{-1} for the hydrazone linkage at pH 7.[36] This suggests that the local environment of the hydrazone extending from the surface of the QD is not dramatically altered compared to bulk solvent.

Since the hydrazone ligation reaction proceeds to near completion, one would expect that the average peptide labeling ratio could be controlled by varying the number of equivalents of *HYNIC* peptide substrate per QD. To test this premise, a batch of QDs (1.1 μM, 1 equiv) was assembled with **1** (16.5 μM, 15 equiv). To this *4FB*-**1**-QD complex, varying equivalents of peptide **2** were added (0, 2, 4, 8, or 12 equiv). Gratifyingly, efficient conversion was achieved, even at a concentration of 2.2 μM of peptide **2** (Table 1). After buffer exchange by gel filtration (PD-10 column) to remove excess aniline, the final ratio of QD/ligated peptide could be calculated by measuring the absorbance at 354 nm (arylhydrazone, QD and TAMRA) and at 555 nm (TAMRA), (Table 1). It is important to note that at the concentrations used, the QD absorbance is low enough ($\varepsilon_{350nm} = 520\,000$ M^{-1} cm^{-1}) to allow for accurate measurements of the hydrazone contribution to the overall absorbance, enabling a quantitative determination of hydrazone formation. For example, the measured hydrazone contribution lowest labeling (two hydrazones at $\varepsilon_{354nm} = 29\,000$ M^{-1} cm^{-1} each) represents $\geq$10% of the total absorbance, which enabled an accurate determination of hydrazone formation.

The physical association of the peptide/QD complex was further confirmed by agarose gel electrophoresis. The QDs used here were surface functionalized with neutral PEG ligands, which means that their migration gel should be slow. We found that the QDs conjugated with an increasing number of peptides migrated faster in the gel, Figure 2. This increase in the mobility shift for the conjugates can be attributed to a net negative charge of the attached peptides. (Although the peptides have equal numbers of positive and negatively charged side chains, there should be a slight net negative charge at pH 8.3.) Also, it is clearly observed (Figure 2, bottom panel) that the fluorescence emitted by the QDs and the TAMRA dye colocalize, and the
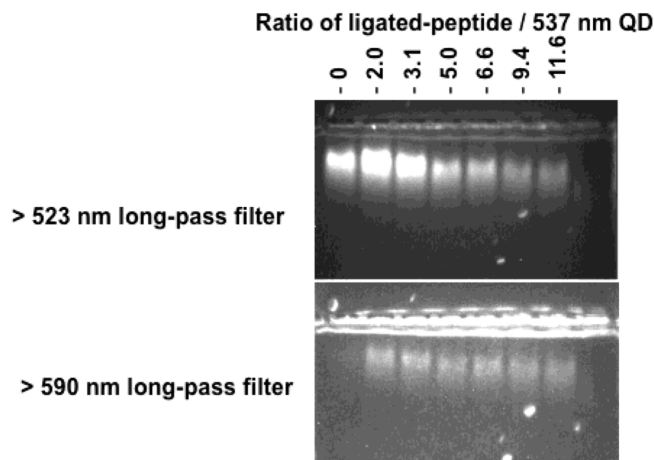
Ratio of ligated-peptide / 537 nm QD

Figure 2. Agarose gel electrophoresis of 537 nm emitting QDs self-assembled with 15-His$_6$-carboxybenzaldehyde peptides after ligation to an increasing ratio of TAMRA substrate peptide as indicated. Using a 523 nm long pass filter allows the simultaneous visualization of the emissions from QDs and TAMRA while use of a 590 nm filter allows only TAMRA signal to be visualized. Note clear evidence of the FRET induced quenching of the QD signal observed when the number of ligated peptides increases (top panel).

emission of the QDs is weaker for bands corresponding to higher peptide **2**/TAMRA ratios (Figure 2, top and bottom panels). This QD PL reduction can be attributed to FRET interactions, which is only possible if both donor (QD) and acceptor (TAMRA) are in close proximity (i.e., QD-peptide **2**-TAMRA conjugate formation). The quenching efficiency increases with the number of TAMRA acceptors per QD up to a 6:1 ratio, and is consistent with the spectroscopic data in Figure 3 (see below). Finally, the integrity of the ligated peptide **3** on the QD was confirmed by gel filtration of the QD/peptide complex, cleavage of the ligated peptides from the QD surface with 0.5 M imidazole and identification by LC/MS (Supporting Information).

FRET Quenching of QDs. The fluorescence emission of each peptide/QD sample clearly displayed evidence of efficient FRET. As shown in Figure 3A, QD donor PL at 537 nm decreases while the sensitized emission of the TAMRA at 587 nm increases in a manner that tracks the ratio of TAMRA attached per QD. An approximately 60% FRET efficiency is measured at a 4:1 TAMRA-peptide/QD ratio; increasing the ratio to 11:1 increases the FRET quenching efficiency to $\sim$80%. These data demonstrate that controlling the peptide/QD ratio is critical for the development of FRET-based sensing of specific biological processes, such proteolytic activity in the present case. Using a quantum yield of 0.2 for the hydrophilic QDs a Förster distance R_0 of $\sim$5 nm is estimated for this donor–acceptor pair[40,51] and analysis of the resulting FRET data (Figure 3B) indicates that the acceptor dye is located at $\sim$5.8 nm from the QD center, which matches the calculated value accounting for the QD radius and peptide extension.[2,19,39,49,52] We should emphasize that the QDs experience a substantial loss in their emission in the presence of the aniline catalyst.[53] Removal of aniline by PD-10 gel filtration lead to a full recovery of QD signal and provided

(51) Pons, T.; Medintz, I. L.; Wang, X.; English, D. S.; Mattoussi, H. *J. Am. Chem. Soc.* **2006**, *128*, 15324–15331.

(52) Mattoussi, H.; Cumming, A. W.; Murray, C. B.; Bawendi, M. G.; Ober, R. *Phys. Rev. B* **1998**, *58*, 7850–7863.

(53) Knowles, K. E.; Tice, D. B.; McArthur, E. A.; Solomon, G. C.; Weiss, E. A. *J. Am. Chem. Soc.* **2010**, *132*, 1041–1050.
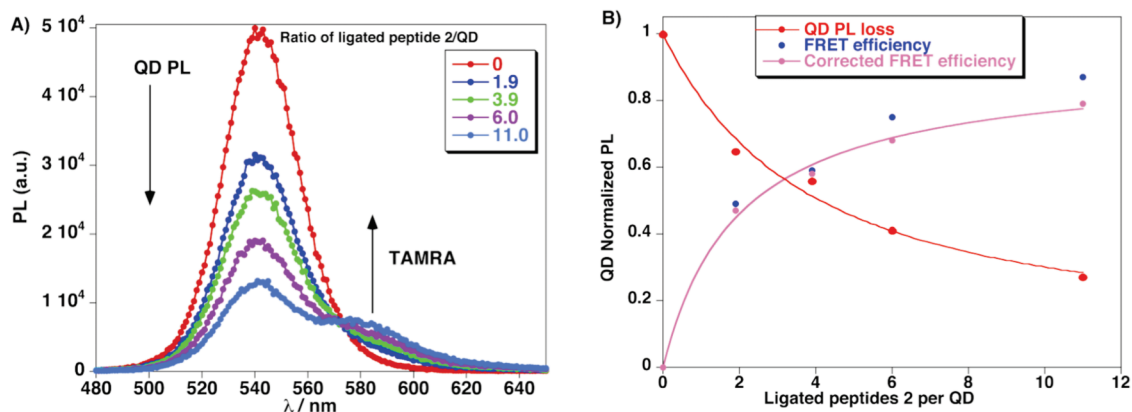
Figure 3. (A) Composite PL spectra of QD-TAMRA-hydrazone peptides **3** conjugates formed from reacting increasing numbers of peptide **2** with QDs preassembled with peptide **1** at (15:1). (B) QD photoluminescence loss (red), FRET efficiency (blue), and FRET efficiency corrected (pink) vs ratio of number of ligated peptides **2** per QD (537 nm) assembled with 15 equiv of peptide **1**.
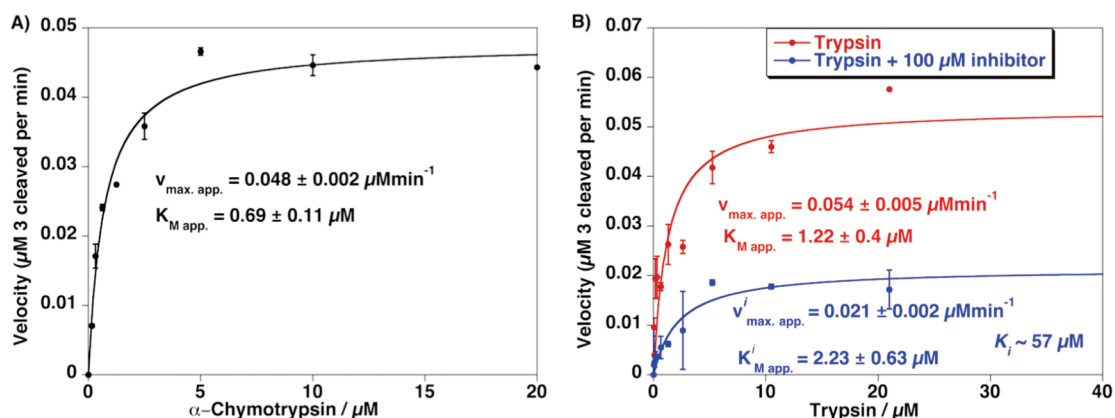

Figure 4. (A) Proteolytic activity from assaying an increasing concentration of chymotrypsin versus a constant amount of QD-TAMRA substrate peptide **3** (0.1 μM QD). Estimated $V_{max.app.}$ and $K_{Mapp.}$ are indicated. (B) Proteolytic activity from assaying an increasing concentration of trypsin versus a constant amount of 537 nm QD-TAMRA substrate peptide **3** (0.1 μM QD) in the absence and presence of 100 μM ovomucoid trypsin inhibitor. Note the change in $V^i_{max.app.}$ while the $K^i_{Mapp.}$ values remain relatively unchanged which is consistent with a competitive inhibition process. K_i value of ~57 μM was estimated from the assay data in the presence of inhibitor. Error bars represent standard deviation from the mean of triplicate measurements.

samples that could be used for the FRET analysis of proteolytic enzyme activity.

Fluorescent Detection of Trypsin and Chymotrypsin. The utility of this new bioconjugation method for QDs was further demonstrated by carrying out enzymatic assays using a ligated peptide on the quantum dot. The TAMRA peptide **3** is a protease substrate that can be cleaved C-terminal to the Arg residue by trypsin or C-terminal to the Tyr residue by chymotrypsin. This cleavage releases the TAMRA dye away from the nanocrystal into bulk solution, reducing the FRET efficiency and which leads to recovery of the QD photoluminescence. The peptide **3**/QD substrate (at an 11:1 ratio) was treated independently with each enzyme by monitoring changes in the fluorescence emission at 537 nm. Using Michaelis−Menten kinetic analysis under the condition of excess enzyme, the maximal apparent velocities $V_{max.app.}$ = 0.048 and 0.054 μM min^{-1} and the Michaelis constants $K_{Mapp.}$ 0.69 and 1.22 μM were determined for α-chymotrypsin and trypsin, respectively (Figure 4).[40,54] The proteolytic ativity of trypsin was monitored in the presence of ovoinhibitor revealing a dissociation constant of K_i ~ 57 μM assuming competitive inhibition. Overall, these results demon-

strate that TAMRA-labeled peptides conjugated to DHLA-PEG$_{600}$ QDs using a Pro$_9$ spacer are sufficiently close to the NP surface to quench the QD luminescence via FRET, yet extend sufficiently beyond the PEG coating to allow for effective proteolytic cleavage. The ability to efficiently couple QDs with control over the QD/substrate ratio, combined with the broad pH stability provided by the DHLA-PEG QD coating, suggests that these NPs may have utility in cellular applications.

Conclusions

A direct and highly efficient ligation strategy using aniline catalyzed hydrazone ligation in neutral aqueous buffer has been demonstrated for attaching peptides to hydrophilic CdSe−ZnS QDs. QD−peptide bioconjugates were prepared in a relatively straightforward manner without use of excess peptide and the resulting labeled NPs were available for use after a single gel filtration step. Importantly, the reactions are highly chemoselective and proceed quantitatively at micromolar concentrations which allows for control over the ratio of peptides ligated per QD; something that is not straightforward using alternative QD-bioconjugation approaches. Further, ratiometric control of peptide valence can be exerted through either the self-assembly of the coating peptide **1** or through the equivalents of *HYNIC*-peptide **2** ligated. The resulting hydrazone linkages have been shown to be stable under physiological conditions including

(54) Medintz, I. L.; Pons, T.; Trammell, S. A.; Grimes, A. F.; English, D. S.; Blanco-Canosa, J. B.; Dawson, P. E.; Mattoussi, H. *J. Am. Chem. Soc.* **2008**, *130*, 16745−16756.

human plasma and absorb uniquely at 354 nm,[55] which enables the monitoring and direct quantitation of peptides attached to QDs. The QD−peptide conjugates assembled using this coupling strategy were further developed as a sensor (via FRET) for the specific detection of proteolysis. This constitutes a major improvement over some of the currently available multistep and difficult to control amide forming reactions. The 'modular' nature of the ligation strategy, that is, interchangeability of functional peptide sequences and linker structure, is an important asset of this approach.

Cumulatively, these remarkable properties suggest aniline catalyzed hydrazone ligation will be a general method for the controlled assembly of a variety of QD-biomolecule hybrids. Since the hydrazone reaction has been shown to be fully chemoselective for all functional groups found in proteins, DNA, and carbohydrates, this approach should find wide utility in QD−biomolecule conjugation.[32] The modular nature of the NP assembly should facilitate optimization of linker length and valency to accommodate these larger biomolecules. In addition, since the ligation reaction is rapid at low micromolar concentrations, biomolecules of limited solubility and large size should be compatible with this strategy, although steric factors may limit the number of macromolecules per QD.

Supporting Information Available: HPLC and MS spectra of the peptides **1**, **2** and **3** (stripped off the QDs), UV and fluorescence spectra of the 537 nm QDs and TAMRA and UV raw trace of the ligation reaction between **1** and **2**. This material is available free of charge via the Internet at http://pubs.acs.org.

JA910988D

(55) Dirksen, A.; Yegneswaran, S.; Dawson, P. E. *Angew. Chem., Int. Ed.* **2010**, *49*, 2023–2027.